

Understanding Higher-Order Correlations Among Semantic Components in Embeddings

Momose Oyama^{1,2} Hiroaki Yamagiwa¹ Hidetoshi Shimodaira^{1,2}

¹Kyoto University ²RIKEN

oyama.momose@sys.i.kyoto-u.ac.jp, hiroaki.yamagiwa@sys.i.kyoto-u.ac.jp,
shimo@i.kyoto-u.ac.jp

Abstract

Independent Component Analysis (ICA) offers interpretable semantic components of embeddings. While ICA theory assumes that embeddings can be linearly decomposed into independent components, real-world data often do not satisfy this assumption. Consequently, non-independencies remain between the estimated components, which ICA cannot eliminate. We quantified these non-independencies using higher-order correlations and demonstrated that when the higher-order correlation between two components is large, it indicates a strong semantic association between them, along with many words sharing common meanings with both components. The entire structure of non-independencies was visualized using a maximum spanning tree of semantic components. These findings provide deeper insights into embeddings through ICA.

1 Introduction

Embeddings play an important role in natural language processing, ranging from word embeddings (Mikolov et al., 2013) to internal representations in language models (Devlin et al., 2019; Brown et al., 2020; Touvron et al., 2023). Understanding how embeddings represent meaning is crucial for unraveling black box NLP models.

Independent Component Analysis (ICA) (Hyvärinen and Oja, 2000) is an effective method for visualizing and interpreting the geometric structure of embeddings (Musil and Mareček, 2024; Yamagiwa et al., 2023). Just as PCA aims to make coordinate axes uncorrelated, ICA seeks to transform the coordinate axes into statistically independent components. The resulting axes from ICA tend to have sparser component values with a few larger values compared to PCA, which increases interpretability as the axes can be seen as specific semantic components (Fig. 1).

However it has been pointed out that the estimated ‘independent components’ are only approxi-

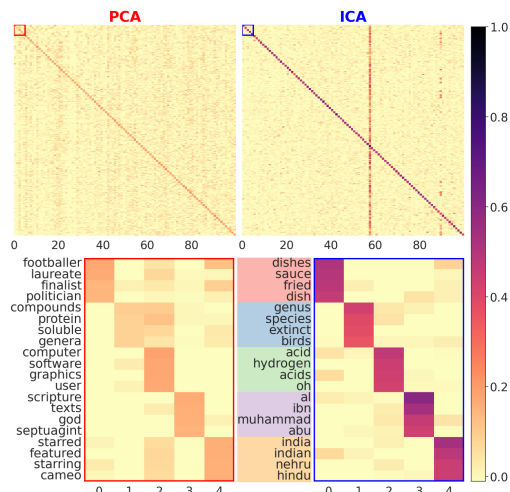


Figure 1: Heatmap visualization of 300-dimensional SGNS embeddings transformed by PCA and ICA, with axes sorted by variance and skewness, respectively. Each embedding has been normalized to have a norm of 1 for better visual interpretation. For each axis, the top 4 words (frequency $n_w \geq 100$ in text8) with largest component values were used. The first 100 axes are displayed in the top panels, and the first 5 axes with the word labels are displayed in the bottom panels. See Appendices A, B and G for details.

mately independent (Hyvärinen et al., 2001; Sasaki et al., 2013, 2014). This is because many real-world datasets cannot be accurately represented as a linear combination of independent components, contradicting the assumption of ICA theory.

In this study, we aim to further interpret the results of applying ICA to embeddings by focusing on the non-independence between ‘independent components’. We measure the degree of non-independence by calculating higher-order correlations between components and find that components with large higher-order correlations can be interpreted as having strong semantic associations. The entire structure is revealed by visualizing the maximum spanning tree of semantic components with higher-order correlations as edge weights.

2 Review: ICA-Transformed Embeddings

Procedure of ICA. For a centered embedding matrix $\mathbf{X} \in \mathbb{R}^{n \times d}$ that represents the meanings of n words by d -dimensional vectors, ICA¹ seeks a transformation $\mathbf{S} = \mathbf{X}\mathbf{B}$ such that each component S_1, \dots, S_d of the transformed matrix $\mathbf{S} = [S_1, \dots, S_d]$ is as statistically independent as possible². The transformation \mathbf{B} can be expressed as the product of the whitening transformation matrix \mathbf{A} (e.g., PCA transformation) and the orthogonal transformation matrix \mathbf{R}_{ica} , i.e., the resulting \mathbf{S} is represented as

$$\mathbf{S} = \mathbf{X}\mathbf{A}\mathbf{R}_{\text{ica}}. \quad (1)$$

Here, \mathbf{R}_{ica} is obtained by minimizing the mutual information³ $I(S_1 \dots S_d) = \sum H(S_i) - H(S_1 \dots S_d)$, which is equivalent to maximizing the non-gaussianity⁴ of the distributions of S_i (Hyvärinen and Oja, 2000). The normalized ICA-transformed embeddings, with each embedding in \mathbf{S} rescaled to a norm of 1, offer high interpretability (Yamagiwa et al., 2023, 2024) and are used for visualizations in this paper.

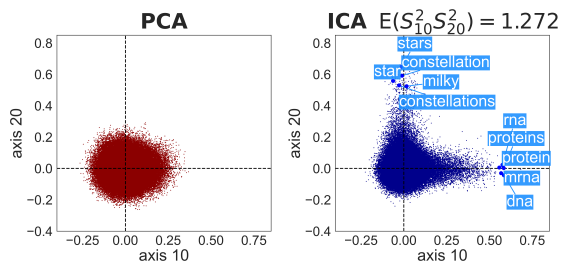


Figure 2: Scatterplots of normalized word embeddings along the 10th and 20th axes. The axes for PCA and ICA-transformed embeddings were arranged in descending order of variance and skewness, respectively. In both transformations, the components are uncorrelated.

Comparison of PCA and ICA. Figure 2 shows that ICA can find the ‘spiky and interpretable shape’ of the embedding distribution (e.g., “biology” and “stars” for the 10th and 20th axes, respectively), but PCA cannot. This is because ICA determines the coordinate axes toward high non-gaussianity, while PCA only considers variance information.

¹For the computation, FastICA (Hyvärinen, 1999) implemented in scikit-learn (Pedregosa et al., 2011) is used.

²The k -th component S_k is also referred to as Axis k .

³ $H(X) = -\int P_X(x) \log P_X(x) dx$ is the entropy.

⁴The degree to which a probability distribution deviates from a Gaussian distribution can be measured using statistics based on higher-order moments, such as skewness (the third moment) or the negentropy of the distribution.

3 Higher-Order Correlations Among Estimated Independent Components

Non-Independence in Real-World Data. The ‘independent components’ estimated by ICA on real-world data are uncorrelated but not completely independent, with dependencies existing between components (Hyvärinen et al., 2001; Sasaki et al., 2013, 2014). This is because ICA assumes a linear decomposition into independent components, an assumption frequently violated in reality.

Higher-Order Correlation. To quantify non-independencies, methods like mutual information and Hilbert-Schmidt Independence Criterion (HSIC) (Gretton et al., 2005) exist. Here we use the higher-order correlation, the simplest measure in terms of computation and formulation. This measure is expressed as follows:

$$E(S_i^2 S_j^2) = \frac{1}{n} \sum_{t=1}^n \mathbf{S}_{t,i}^2 \mathbf{S}_{t,j}^2. \quad (2)$$

Here, \mathbf{S} is the whitened matrix⁵. This can also be interpreted as the covariance between S_i^2 and S_j^2 , plus one, as $\text{cov}(S_i^2, S_j^2) = E((S_i^2 - 1)(S_j^2 - 1)) = E(S_i^2 S_j^2) - 1$. If S_i and S_j are independent of each other, then $E(S_i^2 S_j^2) = E(S_i^2)E(S_j^2) = 1$. Thus, the deviation of $E(S_i^2 S_j^2)$ from 1 is the degree of dependence between S_i and S_j .

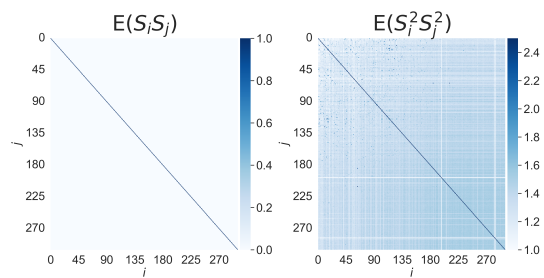


Figure 3: Heatmaps of the correlation coefficient $E(S_i S_j)$ and the higher-order correlation $E(S_i^2 S_j^2)$ of component pairs (S_i, S_j) from ICA on 300-dimensional SGNS embeddings. See Appendix C for details.

Figure 3 shows that the estimated independent components of the embeddings are uncorrelated but not completely independent, with varying degrees of higher-order correlations across pairs. These $E(S_i^2 S_j^2)$ values provide a useful metric of association, as demonstrated in the following section.

⁵The components are (i) centered: $E(S_i) = 0$, the mean of each component is 0, (ii) scaled: $E(S_i^2) = 1$, the variance of each component is 1, and (iii) uncorrelated: $E(S_i S_j) = 0$, the correlations are all zero.

$E(S_0^2 S_{82}^2) = 1.927$		$E(S_6^2 S_{96}^2) = 2.032$		$E(S_{12}^2 S_{66}^2) = 1.975$		$E(S_{16}^2 S_{118}^2) = 2.124$		$E(S_{56}^2 S_{126}^2) = 1.861$		$E(S_{63}^2 S_{210}^2) = 2.964$	
Axis 0	Axis 82	Axis 6	Axis 96	Axis 12	Axis 66	Axis 16	Axis 118	Axis 56	Axis 126	Axis 63	Axis 210
dishes	beer	el	o	rabbi	judah	blood	disorder	cpu	pointer	organization	unesco
sauce	beers	spanish	portuguese	talmud	israelites	organs	mental	microprocessor	return	international	itu
fried	ale	nacional	paulo	rabbis	yahweh	liver	disorders	processor	string	organizations	interpol
dish	brewing	jos	rio	torah	elisha	kidney	symptoms	cpus	pointers	interpol	observer
cooked	yeast	de	portugal	jewish	isaiah	tissue	bipolar	intel	node	standardization	temporary
$E(S_0^2 S_{23}^2) = 0.990$		$E(S_6^2 S_{13}^2) = 0.992$		$E(S_{12}^2 S_{57}^2) = 0.993$		$E(S_{16}^2 S_{57}^2) = 0.996$		$E(S_{56}^2 S_{197}^2) = 0.982$		$E(S_{63}^2 S_{18}^2) = 1.073$	
Axis 0	Axis 23	Axis 6	Axis 13	Axis 12	Axis 57	Axis 16	Axis 57	Axis 56	Axis 197	Axis 63	Axis 18
dishes	statesman	el	windows	rabbi	s	blood	s	cpu	population	organization	actress
sauce	astronomer	spanish	os	talmud	and	organs	and	microprocessor	median	international	footballer
fried	philosopher	nacional	unix	rabbis	was	liver	was	processor	estimated	organizations	musician
dish	johann	jos	linux	torah	in	kidney	in	cpus	residing	interpol	actor
cooked	mathematician	de	microsoft	jewish	by	tissue	by	intel	total	standardization	singer

Table 1: (Top Row) Six randomly selected pairs of components from the top 50 pairs with the highest $|E(S_i^2 S_j^2) - 1|$ values. For each component, the top 5 words (frequency $n_w \geq 100$ in text8) with the largest component values are listed. (Bottom Row) Component pairs with small $E(S_i^2 S_j^2)$ values. For each component S_i with the smaller axis number in the pairs (S_i, S_j) in the top row, a component S_k with the smallest value of $|E(S_i^2 S_k^2) - 1|$ was selected.

	$k = 1$	$k = 2$	$k = 3$	$k = 4$	$k = 5$
List-2 (top- k)	69.0	65.0	64.0	64.5	56.5
List-3 (bottom 30%)	27.0	33.0	32.5	33.5	40.5
Can't decide	4.0	2.0	3.5	2.0	3.0

Table 2: The percentage of each list judged by the GPT model to be more semantically related to List-1.

4 Interpretation of Higher-Order Correlations as Semantic Relevance

4.1 Degree of Semantic Relevance

We show that the values of higher-order correlations $E(S_i^2 S_j^2)$ can be interpreted as the degree of associations between semantic components.

Results: Top Row of Table 1. The meanings of each component, represented by the listed words in component pairs with high $E(S_i^2 S_j^2)$ values, are strongly related. For example, focusing on Axis 0 and Axis 82, a pair with particularly large values of $E(S_i^2 S_j^2)$, we can interpret that Axis 0 has a meaning associated with “dishes” and Axis 82 with “beer”, suggesting that there is a semantic relationship between them.

Results: Bottom Row of Table 1. On the other hand, for component pairs with $E(S_i^2 S_j^2)$ values close to 1, indicating that the components are considered independent, there is no clear relevance between the meanings of the components. For example, looking at the pair of Axis 0 and Axis 23, which has a small $E(S_i^2 S_j^2)$ value, we can interpret that Axis 0 represents “dishes” and Axis 23 represents “polymath”, and there is no direct semantic relationship between them.

Detailed results are shown in Appendix G.

4.2 Quantitative Evaluation via GPT-4o mini

We conducted experiments to quantitatively evaluate whether higher-order correlations between ICA components represent semantic relationships.

Settings. Our experimental procedure was as follows. We first selected the top 100 ICA components, ranked by skewness. For each component i ($i = 0, \dots, 99$), we created three word lists: Word list-1 comprised the top 5 words from component i , Word list-2 contained the top 5 words from the k -th most correlated component with component i ($k = 1, \dots, 5$), and Word list-3 consisted of the top 5 words from a randomly selected low-correlation component (chosen from the bottom 30% of correlated components). Using these lists, we generated pairs (list-1, list-2) and (list-1, list-3), and queried GPT-4o mini to determine which pair was more semantically related⁶. This procedure was executed for all 100 components, resulting in 200 total comparisons for each value of k from 1 to 5. The specific prompt used for GPT-4o mini model is provided in Appendix D.

Results and Discussion. Table 2 shows the result of the experiment. We can see that component pairs with higher-order correlations tend to be more semantically related (69.0% for $k = 1$ vs 27.0% for bottom 30%), and that semantic relatedness gradually declines as correlation decreases (69.0% at $k = 1$ to 56.5% at $k = 5$). These results quantitatively demonstrate that higher-order correlations between ICA components effectively reflect semantic relatedness between corresponding words.

⁶To mitigate potential biases, we randomly shuffled the order of the lists in the pairs and repeated this process with the reversed order: (list-1, list-3) and (list-1, list-2).

$E(S_{10}^2, S_2^2) = 2.323$		$E(S_{10}^2, S_{16}^2) = 1.947$		$E(S_{10}^2, S_{160}^2) = 1.811$		$E(S_{27}^2, S_{11}^2) = 1.643$		$E(S_{27}^2, S_{64}^2) = 1.997$		$E(S_{27}^2, S_{104}^2) = 1.605$	
Axis 10	Axis 2	Axis 10	Axis 16	Axis 10	Axis 160	Axis 27	Axis 11	Axis 27	Axis 64	Axis 27	Axis 104
dna	acid	dna	blood	dna	evolution	greek	gaius	greek	goddess	greek	archaeological
proteins	hydrogen	proteins	organs	proteins	evolutionary	greece	caesar	greece	gods	greece	neolithic
rna	acids	rna	liver	rna	darwin	athens	augustus	athens	deity	athens	bc
mrna	oh	mrna	kidney	mrna	selection	athenian	lucius	athenian	deities	athenian	pottery
w_k	$S_{k,10}^2 S_{k,2}^2$	w_k	$S_{k,10}^2 S_{k,16}^2$	w_k	$S_{k,10}^2 S_{k,160}^2$	w_k	$S_{k,27}^2 S_{k,11}^2$	w_k	$S_{k,27}^2 S_{k,64}^2$	w_k	$S_{k,27}^2 S_{k,104}^2$
ribose	3755.7	adenylate	2079.8	utr	2381.5	laertius	898.3	demeter	2348.5	tiryns	1690.6
deoxyribose	2963.9	effectors	1842.5	reticulum	1942.0	preveza	788.0	hephaestus	2204.3	knossos	1348.1
phosphodiester	2850.2	antisense	1639.9	genomic	1668.6	xanthippus	764.2	hestia	2021.5	mycenaean	1205.6
biosynthesis	2510.1	cyclase	1638.9	homozygous	1599.1	rhadamanthus	735.5	hera	1744.6	lending	1124.7
methyltransferase	2482.9	myosin	1201.8	cleaved	1181.0	thracians	711.8	cronos	1720.2	hissarlik	1103.1
pyrimidine	2399.6	axons	1144.2	tubulin	1152.4	alexandri	705.2	aphrodite	1675.9	melos	1006.3

Table 3: For 6 component pairs (S_i, S_j) selected from adjacent component pairs in the MST defined in Sec. 5, the top 6 words and their corresponding $S_{t,i}^2 S_{t,j}^2$ values that contribute the most to the $E(S_i^2 S_j^2)$ value are shown.

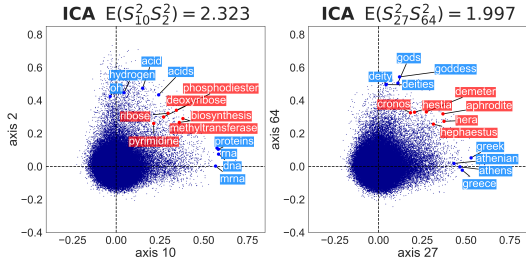


Figure 4: Scatter plots of normalized word embeddings for axis pairs (10, 2) and (27, 64) with large values of higher-order correlations. Blue-labeled words are the top 4 words for each axis’s component values, while red-labeled words are the top 6 words for the values of $S_{t,i}^2 S_{t,j}^2$. See Appendix C for all the pairs in Table 3.

4.3 Decomposition of Semantic Relevance

For a component pair (S_i, S_j) , words w_t with large values of $S_{t,i}^2 S_{t,j}^2$ are considered to make a significant contribution to the higher-order correlation $E(S_i^2 S_j^2) = \frac{1}{n} \sum_{t=1}^n S_{t,i}^2 S_{t,j}^2$. Here we investigate words that significantly contribute to the $E(S_i^2 S_j^2)$ values and gain a more concrete understanding of the relationships between components.

Results. Table 3 presents component pairs selected from the maximum spanning tree T_{150} (Sec. 5) and words significantly contributing to their $E(S_i^2 S_j^2)$ values. These words often relate to the meanings of both components, demonstrating additive compositionality. For example, in the Axis 10 and Axis 2 pair, words like *ribose*, *deoxyribose*, *phosphodiester*, *biosynthesis*, *methyltransferase*, and *pyrimidine* notably contribute to the $E(S_i^2 S_j^2)$ value, linking biomolecules and chemical components. Detailed results are shown in Appendix G.

Visualization. Figure 4 shows word embedding scatter plots for axis pairs (10, 2) and (27, 64) with large higher-order correlations to illustrate the distribution of words with significant contributions

to higher-order correlations. Unlike a typical independent component scatter plot (Fig. 2), these exhibit many words with large component values in both axes, reflecting the meanings of both axes and demonstrating the additive compositionality of embeddings. For the (10, 2) pair, words that notably contribute to the $E(S_i^2 S_j^2)$ (*ribose*, *deoxyribose*, *phosphodiester*, *biosynthesis*, *methyltransferase*, and *pyrimidine*) appear with significant values in both components. This abundance of words sharing both semantic components is characteristic of pairs with large higher-order correlations. Detailed results are shown in Appendix C.

5 Visualization of Non-Independence Structure

In this section, we construct a maximum spanning tree (MST) based on higher-order correlations to visualize the non-independence between estimated independent components.

Settings. The 300 ICA components, originally ordered by skewness with $i = 0, \dots, 299$, were re-sorted in descending order of semantic component consistency scores to prioritize axes that are more easily interpretable as specific semantic components. The semantic component consistency scores were determined by a word intrusion task (Chang et al., 2009). A higher consistency score indicates easier interpretability. Details of the scoring methods are provided in Appendix E.1. We introduce the notation σ to map the order of consistency scores to the original axis numbers in the skewness order: $\sigma(j)$ represents the axis number in the skewness sort for the axis with the j -th highest consistency score. Then, we consider a weighted complete graph G_{150} , with 150 components having high consistency scores $S_{\sigma(i)}$ ($i \in 0, \dots, 149$) as nodes. For the edge between the node pair (S_i, S_j) ,

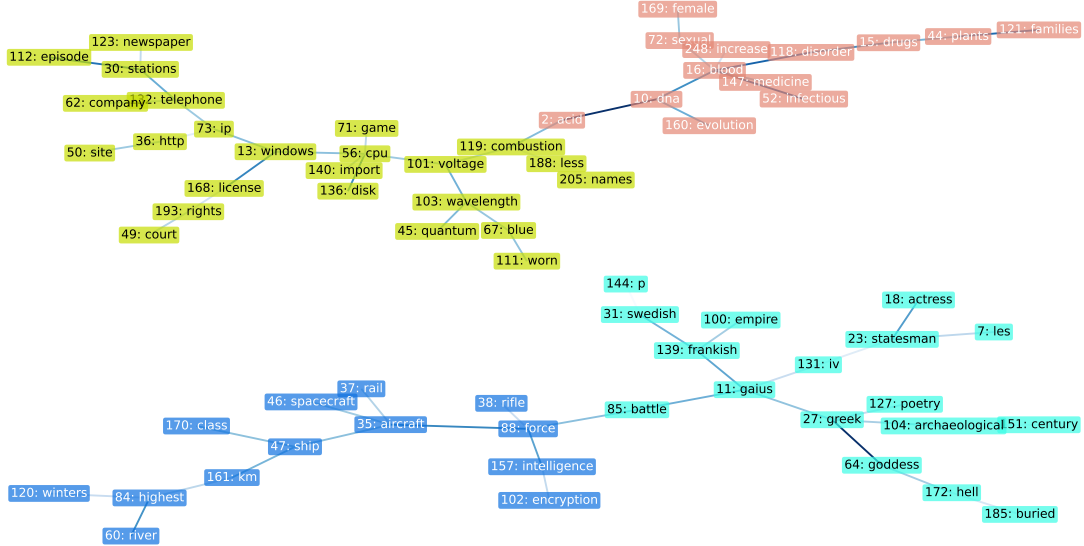


Figure 5: Subtrees of MST T_{150} defined in Sec. 5. Each node represents an independent component S_k (i.e., Axis k) estimated by ICA. The label of each node is “ k : TopWord(k)”, where TopWord(k) is the word with the largest component value along axis k among words with frequency $n_w \geq 100$ in the text8 corpus. The color of the edge between nodes (i, j) represents the magnitude of the $E(S_i^2 S_j^2)$ value between the components, with darker edge colors indicating larger values.

we set $c_{ij} = E(S_i^2 S_j^2)$ as the weight. To visualize and interpret G_{150} , we compute the maximum spanning tree (MST)⁷ T_{150} , a spanning tree that maximizes the sum of c_{ij} in the graph G_{150} . MST was relatively more interpretable than other subgraphs of graph G_{150} , providing a good balance between visibility and element relationships.

Interpretation of the MST. The MST T_{150} represents a graph structure expressing the non-independence between estimated independent components. Since the edges in T_{150} connect component pairs with large higher-order correlations, we can interpret that there is a strong relationship between the components connected by these edges. Furthermore, the subtrees of T_{150} represent groups of semantically related components, and the components within these groups tend to have similar meanings.

Results and Discussion. Figure 5 shows a part of the MST T_{150} ; the entire MST T_{150} is exhibited in Appendix E.2. The colors correspond to the clusters obtained by applying spectral clustering⁸ (Ng et al., 2001) to T_{150} . The weights used for clustering are the higher-order correlations. From

the MST, we can infer structures such as connections and groupings of meanings among three or more components⁹. For example, semantically related component pairs such as (2: *dna*, 10: *acid*) in the pink cluster and (27: *greek*, 64: *goddess*) in the cyan cluster are connected by edges in T_{150} . Additionally, groups such as {168: *license*, 13: *windows*, 56: *cpu*} in the yellow cluster and {46: *spacecraft*, 35: *aircraft*, 47: *ship*} in the blue cluster form semantic clusters as sets of nodes connected by edges. The components within these groups can be interpreted as having meanings related to “computer” and “vehicle”, respectively.

6 Conclusion

Both ICA and PCA transformations make the components uncorrelated. ICA goes further by making the components nearly independent, but some non-independence still remains. In this study, we used higher-order correlations to quantify the non-independence between the components in the ICA-transformed word embeddings. By interpreting these as the semantic associations between the components and visualizing the overall structure, we can gain a deeper understanding of the latent semantic structure within the embeddings.

⁷We used `minimum_spanning_tree` implemented in NetworkX (Hagberg et al., 2008) for the computation of the MST. See Appendix E.2 for details.

⁸We used `SpectralClustering` implemented in scikit-learn (Pedregosa et al., 2011).

⁹Furthermore, in Appendix F, we conducted a dimensionality reduction experiment that numerically demonstrates how the MST effectively represents a significant structure among the components.

Limitations

- The embeddings used in the experiments are limited to SGNS word embeddings. For a more thorough analysis, it is necessary to conduct experiments using various types of embeddings.
- For large embedding matrices with a high number of data points n , ICA may fail to converge within a practical timeframe. To overcome this, we suggest using subsampled data to estimate the ICA transformation matrix, which can then be applied to unseen embedding vectors.
- When n is large, calculating higher-order correlations (eq. 2) may become computationally intensive. This calculation is similar to the computation of the variance-covariance matrix and can be approximated by subsampling data points. Further speedup can be achieved by parallelization of the computation.
- Since ICA leverages the non-Gaussianity of embedding distributions, it is not suitable for analysis if the original embeddings follow a multivariate Gaussian distribution.

Ethics Statement

This study complies with the [ACL Ethics Policy](#).

Acknowledgements

This study was partially supported by JSPS KAKENHI 22H05106, 23H03355, JST CREST JPMJCR21N3, JST BOOST JPMJBS2407, JST SPRING JPMJSP2110.

Code Availability

Code is available at <https://github.com/momoseoyama/hoc>.

References

- Tom Brown, Benjamin Mann, Nick Ryder, Melanie Subbiah, Jared D Kaplan, Prafulla Dhariwal, Arvind Neelakantan, Pranav Shyam, Girish Sastry, Amanda Askell, Sandhini Agarwal, Ariel Herbert-Voss, Gretchen Krueger, Tom Henighan, Rewon Child, Aditya Ramesh, Daniel Ziegler, Jeffrey Wu, Clemens Winter, Chris Hesse, Mark Chen, Eric Sigler, Mateusz Litwin, Scott Gray, Benjamin Chess, Jack Clark, Christopher Berner, Sam McCandlish, Alec Radford, Ilya Sutskever, and Dario Amodei. 2020.
- Language models are few-shot learners. In *Advances in Neural Information Processing Systems*33: Annual Conference on Neural Information Processing Systems 2020, *NeurIPS*, pages 1877–1901.
- Elia Bruni, Nam-Khanh Tran, and Marco Baroni. 2014. Multimodal distributional semantics. *Journal of Artificial Intelligence Research*, 49:1–47.
- Jonathan Chang, Sean Gerrish, Chong Wang, Jordan Boyd-graber, and David Blei. 2009. [Reading tea leaves: How humans interpret topic models](#). In *Advances in Neural Information Processing Systems*, volume 22. Curran Associates, Inc.
- Jacob Devlin, Ming-Wei Chang, Kenton Lee, and Kristina Toutanova. 2019. [BERT: Pre-training of deep bidirectional transformers for language understanding](#). In *Proceedings of the 2019 Conference of the North American Chapter of the Association for Computational Linguistics: Human Language Technologies, Volume 1 (Long and Short Papers)*, pages 4171–4186, Minneapolis, Minnesota. Association for Computational Linguistics.
- Lev Finkelstein, Evgeniy Gabrilovich, Yossi Matias, Ehud Rivlin, Zach Solan, Gadi Wolfman, and Eytan Ruppin. 2002. Placing search in context: The concept revisited. *ACM Transactions on information systems*, 20(1):116–131.
- Daniela Gerz, Ivan Vulić, Felix Hill, Roi Reichart, and Anna Korhonen. 2016. SimVerb-3500: A large-scale evaluation set of verb similarity. In *Proceedings of the 2016 Conference on Empirical Methods in Natural Language Processing*, pages 2173–2182.
- Arthur Gretton, Olivier Bousquet, Alex Smola, and Schölkopf Bernhard. 2005. Measuring statistical dependence with hilbert-schmidt norms. In *The International Conference on Algorithmic Learning Theory, ALT*, pages 63–77.
- Aric A Hagberg, Daniel A Schult, and Pieter J Swart. 2008. Exploring network structure, dynamics, and function using networkx. *Proceedings of the 7th Python in Science Conference (SciPy 2008)*, pages 11–15.
- Felix Hill, Roi Reichart, and Anna Korhonen. 2015. Simlex-999: Evaluating semantic models with (genuine) similarity estimation. *Computational Linguistics*, 41(4):665–695.
- Aapo Hyvärinen. 1999. Fast and robust fixed-point algorithms for independent component analysis. *IEEE Transactions on Neural Networks*, 10(3):626–634.
- Aapo Hyvärinen, Patrik O. Hoyer, and Mika Inki. 2001. Topographic independent component analysis. *Neural Computation*, 13(7):1527–1558.
- Aapo Hyvärinen and Erkki Oja. 2000. Independent component analysis: Algorithms and applications. *Neural networks*, 13(4-5):411–430.

Thang Luong, Richard Socher, and Christopher Manning. 2013. Better word representations with recursive neural networks for morphology. In *Proceedings of the Seventeenth Conference on Computational Natural Language Learning*, pages 104–113.

Matt Mahoney. 2011. About the test data. <http://matmahoney.net/dc/textdata.html>.

Tomás Mikolov, Ilya Sutskever, Kai Chen, Greg Corrado, and Jeffrey Dean. 2013. Distributed representations of words and phrases and their compositionality. In *Advances in Neural Information Processing Systems 26: Annual Conference on Neural Information Processing Systems 2013, NeurIPS*, pages 3111–3119.

Tomáš Musil and David Mareček. 2024. Exploring interpretability of independent components of word embeddings with automated word intruder test. In *Proceedings of the 2024 Joint International Conference on Computational Linguistics, Language Resources and Evaluation (LREC-COLING 2024)*, pages 6922–6928, Torino, Italia. ELRA and ICCL.

Andrew Ng, Michael Jordan, and Weiss. 2001. On spectral clustering: Analysis and an algorithm. In *Advances in Neural Information Processing Systems 14: Annual Conference on Neural Information Processing Systems 2001, NIPS*.

Fabian Pedregosa, Gaël Varoquaux, Alexandre Gramfort, Vincent Michel, Bertrand Thirion, Olivier Grisel, Mathieu Blondel, Peter Prettenhofer, Ron Weiss, Vincent Dubourg, Jake Vanderplas, Alexandre Passos, David Cournapeau, Matthieu Brucher, Matthieu Perrot, and Édouard Duchesnay. 2011. Scikit-learn: Machine learning in python. *Journal of Machine Learning Research*, 12(85):2825–2830.

Kira Radinsky, Eugene Agichtein, Evgeniy Gabrilovich, and Shaul Markovitch. 2011. A word at a time: Computing word relatedness using temporal semantic analysis. In *Proceedings of the 20th International Conference on World Wide Web*, page 337–346.

Hiroaki Sasaki, Michael Gutmann, Hayaru Shouno, and Aapo Hyvärinen. 2013. Correlated topographic analysis: estimating an ordering of correlated components. *Machine Learning*, 92:285–317.

Hiroaki Sasaki, Michael Gutmann, Hayaru Shouno, and Aapo Hyvärinen. 2014. Estimating Dependency Structures for non-Gaussian Components with Linear and Energy Correlations. In *Proceedings of the Seventeenth International Conference on Artificial Intelligence and Statistics, AISTATS*, pages 868–876.

Fei Sun, J. Guo, Yanyan Lan, Jun Xu, and Xueqi Cheng. 2016. Sparse word embeddings using l_1 regularized online learning. In *International Joint Conference on Artificial Intelligence*.

Hugo Touvron, Louis Martin, Kevin Stone, Peter Albert, Amjad Almahairi, Yasmine Babaei, Nikolay Bashlykov, Soumya Batra, Prajwal Bhargava, Shruti

Bhosale, et al. 2023. Llama 2: Open foundation and fine-tuned chat models. *arXiv preprint arXiv:2307.09288*.

Hiroaki Yamagiwa, Momose Oyama, and Hidetoshi Shimodaira. 2023. Discovering universal geometry in embeddings with ICA. In *Proceedings of the 2023 Conference on Empirical Methods in Natural Language Processing*, pages 4647–4675, Singapore. Association for Computational Linguistics.

Hiroaki Yamagiwa, Momose Oyama, and Hidetoshi Shimodaira. 2024. Revisiting cosine similarity via normalized ica-transformed embeddings. *arXiv preprint arXiv:2406.10984*.

A Details of Experimental Settings

The word embeddings used in the experiments were trained using Skip-gram with Negative Sampling (SGNS). The parameters used to train SGNS are summarized in Table 4. The corpus used for training is the text8 corpus (Mahoney, 2011), and the number of vocabulary words is $n = 253,854$.

Dimensionality	300
Epochs	100
Window size h	10
Negative samples ν	5
Learning rate	0.025
Min count	1

Table 4: SGNS parameters.

B Remarks on Axis 57 in Figure 1

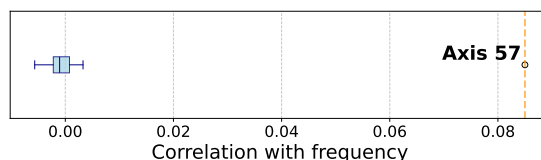


Figure 6: Boxplot of correlation coefficients between word frequency n_w and the component values for the 0th to 99th axes of the ICA-transformed embeddings. Axis 57 shows a particularly high correlation coefficient.

An interesting vertical streak is observed in Axis 57 of the heatmap for ICA-transformed embeddings in Fig. 1. This streak can be explained by several factors. As shown in Fig. 6, Axis 57 exhibits a strong correlation between component values and word frequencies n_w , suggesting that Axis 57 is more associated with word frequency than with a specific semantic meaning. Additionally, the words used in Fig. 1 were selected from those appearing more than 100 times in the text8 corpus, resulting in a bias towards high-frequency

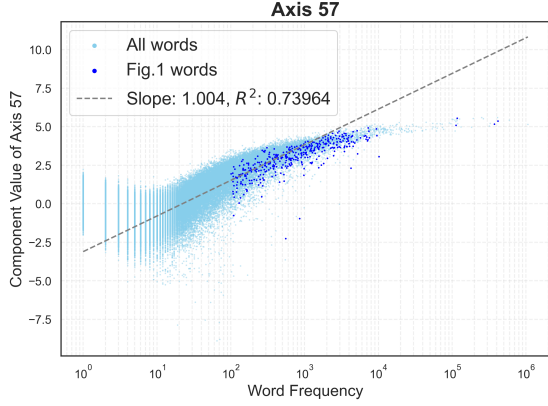


Figure 7: Scatter plot of word frequency n_w versus the component values of the 57th axis of the ICA-transformed embeddings. Words used in Fig. 1 are highlighted in dark blue. The regression line and coefficient of determination were calculated for words with a frequency of $n_w \geq 10$.

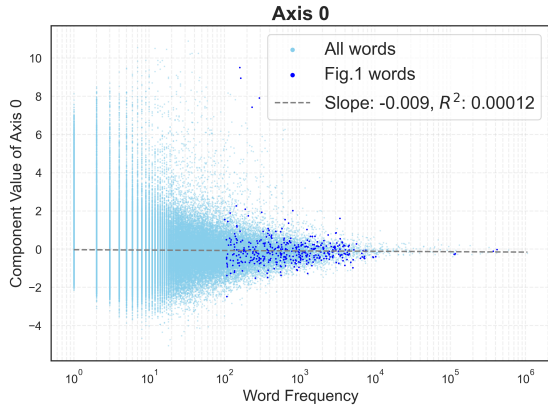


Figure 8: Scatter plot of word frequency n_w versus the component values of the 0th axis of the ICA-transformed embeddings. The settings are the same as in Fig. 7.

words. This tendency is further illustrated in Fig. 7, which demonstrates that words used in the heatmap ($n_w \geq 100$) tend to have larger component values along Axis 57. In contrast, Fig. 8 shows that for axes with weak correlation to word frequency, the words used in the heatmap do not exhibit notably large component values. Consequently, large component values were observed along Axis 57 in the heatmap, a pattern that was unique to Axis 57 and not observed in other axes.

C Higher-Order Correlations

C.1 Distribution of Higher-Order Correlations

Figures 9a and 9b show histograms of higher-order correlations $E(S_i^2 S_j^2)$ for pairs where $i < j$ and

for all pairs including $E(S_i^4)$ where $i = j$, respectively. While there are component pairs where $E(S_i^2 S_j^2) < 1$, in Fig. 3, the range of values was truncated between 1.0 and 2.5 for visualization purposes.

C.2 Scatterplots for Independent Axes

Complementary Results for Sec. 4.3. Table 3 in Sec. 4.3 presented words with significant contributions to higher-order correlations for six axis pairs. While the main text illustrated the distribution of these highly contributing words through scatter plots for the two selected pairs, Figure 10 provides scatter plots for all the six pairs.

The Relationship Between the Magnitude of Higher-Order Correlations and the Appearance of Scatter Plots.

Figure 11 presents the scatter plots of word embeddings for 24 component pairs, each with different higher-order correlation values. We can see that as the magnitude of higher-order correlation increases, the number of words with large component values along both axes increases as well. The selection of these 24 pairs was conducted as follows: First, we considered 150 components $S_{\sigma(0)}, \dots, S_{\sigma(149)}$ with high semantic consistency (see Appendix E.1 for the calculation method). We then sorted all possible component pairs (S_i, S_j) ($i, j \in \sigma(0), \dots, \sigma(149)$) based on the value of $|E(S_i^2 S_j^2) - 1|$. We established 24 equally spaced grids between the minimum and maximum values, and selected pairs closest to each grid point without repetition.

Words with Significant Contributions to Higher-Order Correlations.

We have observed words with significant contributions, i.e., with large values of $S_{t,i}^2 S_{t,j}^2$, to higher-order correlations $E(S_i^2 S_j^2)$ in Table 3 in Sec. 4.3, and will see further examples in Tables 8 and 9 in Appendix G. Such words are labeled in red in the scatter plots in Fig. 4 in Section 4.3, as well as in Figs. 10 and 11 in Appendix C.2. For axis pairs with large higher-order correlations, we observe a large number of words that make significant contributions to the higher-order correlations. The meanings of these words include both axes' meanings, demonstrating the additive compositionality of embeddings.

D Prompt Used for Evaluation by GPT-4o mini

The specific prompt used for the GPT-4o mini model is provided below.

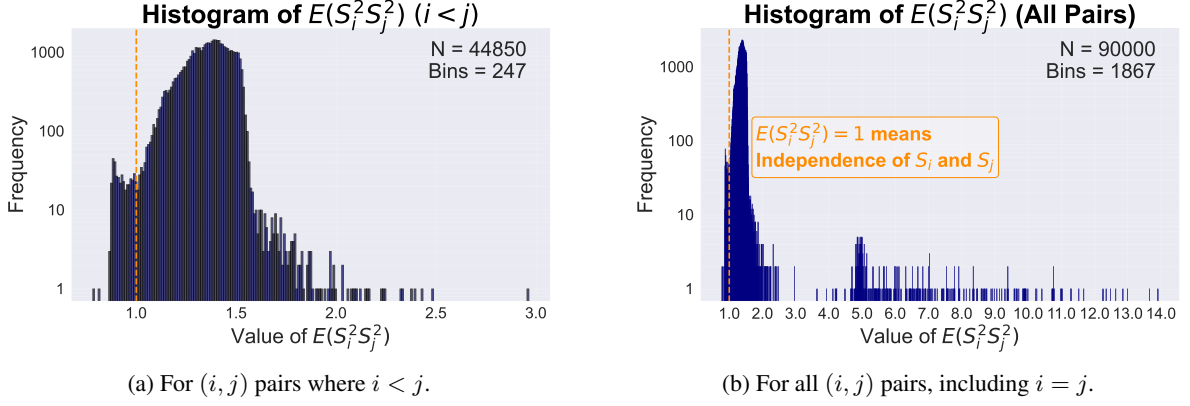


Figure 9: Histograms of higher-order correlations.

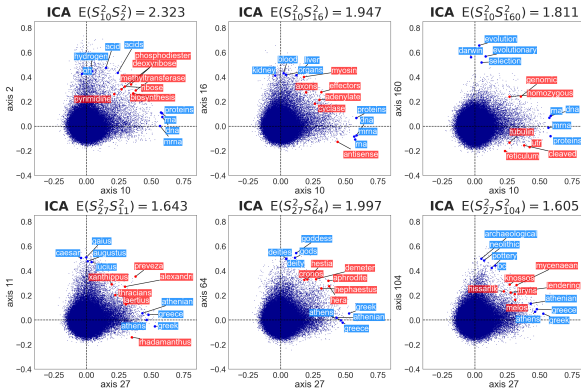


Figure 10: Scatter plots of normalized word embeddings for axis pairs in Table 3. Blue-labeled words are the top 4 words for each axis’s component values, while red-labeled words are the top 6 words for values of $S_{t,i}^2 S_{t,j}^2$.

Question:
 You are given 2 list pairs (A, B), (C, D).
 If one pair is more semantically relevant than the other, answer the pair.
 If you cannot determine, answer "XX".

List pair (A, B): ({wordlist_1}, {wordlist_2})
 List pair (C, D): ({wordlist_1}, {wordlist_3})

Output:
 "AB" if (A, B) is more semantically related
 "CD" if (C, D) is more semantically related
 "XX" if equally related, or you can't decide
 Respond with only AB, CD, or XX.

When conducting the experiment, we took the following steps to eliminate any potential biases arising from the order of word sequences and specific label names.

1. To remove the influence of word order within lists, we randomly shuffled the words in wordlist_1, wordlist_2, and wordlist_3.
2. To prevent bias in output labels, we conducted the experiment twice, swapping wordlist_2 and wordlist_3 between runs.

3. To account for order bias in the prompt, we randomly alternated the order of the following two lines:

```
List pair (A, B): ({wordlist_1}, {wordlist_2})
List pair (C, D): ({wordlist_1}, {wordlist_3})
```

E Details of Visualization of Non-Independence Structure

E.1 Scoring ICA Axes: Word Intrusion Task

We assigned a semantic coherence score to each axis of the ICA-transformed embeddings using the word intrusion task method (Chang et al., 2009).

Word Intrusion Task. The word intrusion task is a method used to evaluate the semantic coherence of a set of k words by assessing the ability to identify an intruder word. For instance, consider the set of words $\{windows, os, unix, linux, microsoft\}$, which has a consistent theme of operating systems. In this case, an unrelated word such as *waterskiing* should be easily identifiable as an intruder, as it does not align with the theme of operating systems. In our experiment, we assigned coherence scores to the top $k = 5$ words (with frequency $n_w \geq 100$ in the text8 corpus) for each axis.

Selection of the Intruder Word. In order to select the intruder word for the set of top k words of each axis $a \in \{1, \dots, d\}$, denoted as $\text{top}_k(a)$, we randomly chose a word from a pool of words that satisfy both of the following criteria simultaneously: (i) the word ranks in the lower 50% in terms of the component value on the axis a , and (ii) it ranks in the top 10% in terms of the component value on some axis other than a . For each axis, $L = 100$ intruder words are randomly selected, and $W_{\text{int}}(a)$ denotes the set of these L intruder words.

Scoring Method. For the consistency score of the meaning of each axis a , $\text{Score}(a)$, we adopted the metric proposed by Sun et al. (2016).

$$\text{Score}(a) = \frac{\text{InterDist}(a)}{\text{IntraDist}(a)}$$

$$\text{IntraDist}(a) = \sum_{\substack{w_i, w_j \in \text{top}_k(a) \\ w_i \neq w_j}} \frac{\text{dist}(w_i, w_j)}{k(k-1)}$$

$$\text{InterDist}(a) = \text{mean}_{w \in W_{\text{int}}(a)} \sum_{w_i \in \text{top}_k(a)} \frac{\text{dist}(w_i, w)}{k}$$

In this formula, we defined $\text{dist}(w_i, w_j) = \|s_i - s_j\|$ for the ICA-transformed embeddings. Here, $\text{IntraDist}(a)$ denotes the average distance between the top k words, and $\text{InterDist}(a)$ represents the average distance between the top words and the intruder words. The score is higher when the intruder words are further away from the set $\text{top}_k(a)$. Therefore, this score serves as a quantitative measure of the ability to identify the intruder word, thus it is used as a measure of the consistency of the meaning of the top k words and the interpretability of axes.

E.2 Entire Visualization of MST

Figure 12 is the visualization of maximum spanning tree (MST) T_{150} defined in Sec. 5. For a graph G_{150} , where the cost between nodes i and j defined as $c_{ij} = E(S_i^2 S_j^2)$, the algorithm to find the MST T is a greedy method that maximizes the total sum of costs, $\sum_{(i,j) \in T} c_{ij}$, subject to T being a spanning tree. The greedy algorithm selects edges in decreasing order of c_{ij} while adhering to the tree constraint. Due to the monotonicity of $f(x) = 1/x$, the decreasing order of c_{ij} is equivalent to the increasing order of $1/c_{ij}$. Thus, computing the MST T_{150} in the graph G_{150} is equivalent to finding the minimum spanning tree, which minimizes the sum of $1/c_{ij}$.

F Dimensionality Reduction via MST

	$d=2$	$d=5$	$d=10$	$d=20$	$d=50$	$d=100$
Random Clustering on components (PCA)	0.04	0.08	0.12	0.16	0.23	0.29
Random Clustering on components (ICA)	0.04	0.08	0.12	0.17	0.24	0.29
Spectral Clustering on MST (PCA)	0.03	0.08	0.13	0.17	0.24	0.30
Spectral Clustering on MST (ICA)	0.06	0.13	0.18	0.23	0.28	0.31

Table 5: Word similarity scores for dimensionality reduction.

We experimentally confirmed that the structure of higher-order correlations between components

can be applied to the dimensionality reduction of embeddings. Specifically, we performed Spectral Clustering on the maximum Spanning Tree (MST) T_{300} , which was computed based on the higher-order correlations between components. By reducing the dimensionality of the embeddings through averaging the clustered axes, we verified that the accuracy degradation in Word Similarity Tasks was mitigated compared to random clustering.

Experimental Settings. We conducted our experiments using the 300-dimensional word embeddings (SGNS). These embeddings were subjected to PCA and ICA to obtain components for clustering. We employed two clustering methods: (1) Random Clustering and (2) Spectral Clustering on the maximum Spanning Tree (MST) T_{300} , which was computed based on the higher-order correlations calculated using Eq. 2. Clustering was performed with the number of clusters ranging from 2 to 100. Dimensionality reduction was achieved by averaging the clustered axes, resulting in reduced dimensions from $d = 2$ to $d = 100$. The performance of the lower-dimensional embeddings was evaluated through Word Similarity Tasks. For the Word Similarity Tasks, we utilized six datasets: MEN (Bruni et al., 2014), WS353 (Finkelstein et al., 2002), MTurk (Radinsky et al., 2011), RW (Luong et al., 2013), SimLex999 (Hill et al., 2015), and SimVerb3500 (Gerz et al., 2016). Each dataset comprises word pairs along with gold similarity scores, assigned by human annotators. We employed the Spearman rank correlation coefficient between human ratings and the cosine similarity of the word embeddings as the evaluation metric. The reported values represent the average scores across the six datasets.

Results and Discussion The experimental results are presented in Table 5. We observe that ICA-based methods outperform PCA-based methods. Moreover, our proposed method, Spectral Clustering on the MST of ICA components, consistently achieves the best performance across all dimensions. This can be attributed to the fact that components included in the same cluster on the MST likely have high semantic relevance and play similar roles in representing the meaning of words. These results validate that considering higher-order correlations between axes better preserves semantic relationships in compressed word embeddings, demonstrating the practical utility of our method. It is important to note that this evaluation assesses the

performance of clustering using a downstream task of dimensionality reduction, rather than dimensionality reduction itself.

G Supplementary Tables for ICA Components and MST Subtrees

Table 6 shows all components of the ICA-transformed word embeddings used in our experiments. Associated with the experiments in Sec. 4.1, Table 7 shows the top 60 pairs with the highest $E(S_i^2 S_j^2)$ values. Additionally, in Table 8 and Table 9, we report on all component pairs in the subtrees of MST T_{150} shown in Fig. 5, extending the results from the selected pairs previously reported in Sec. 4.3.

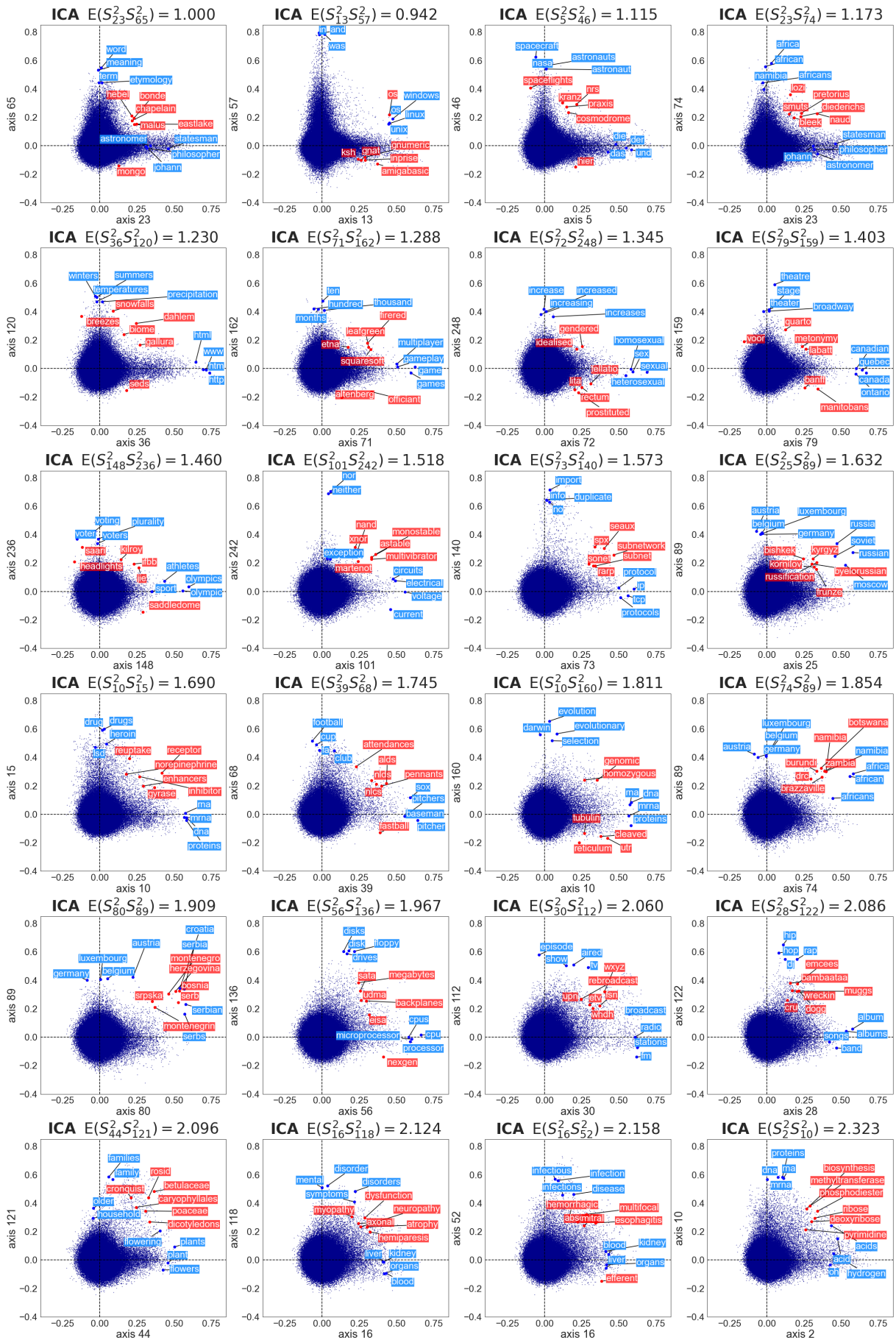


Figure 11: Scatter plots of normalized word embeddings for 24 axis pairs. Blue-labeled words are the top 4 words for each axis's component values, while red-labeled words are the top 6 words for values of $S^2_{t,i} S^2_{t,j}$.

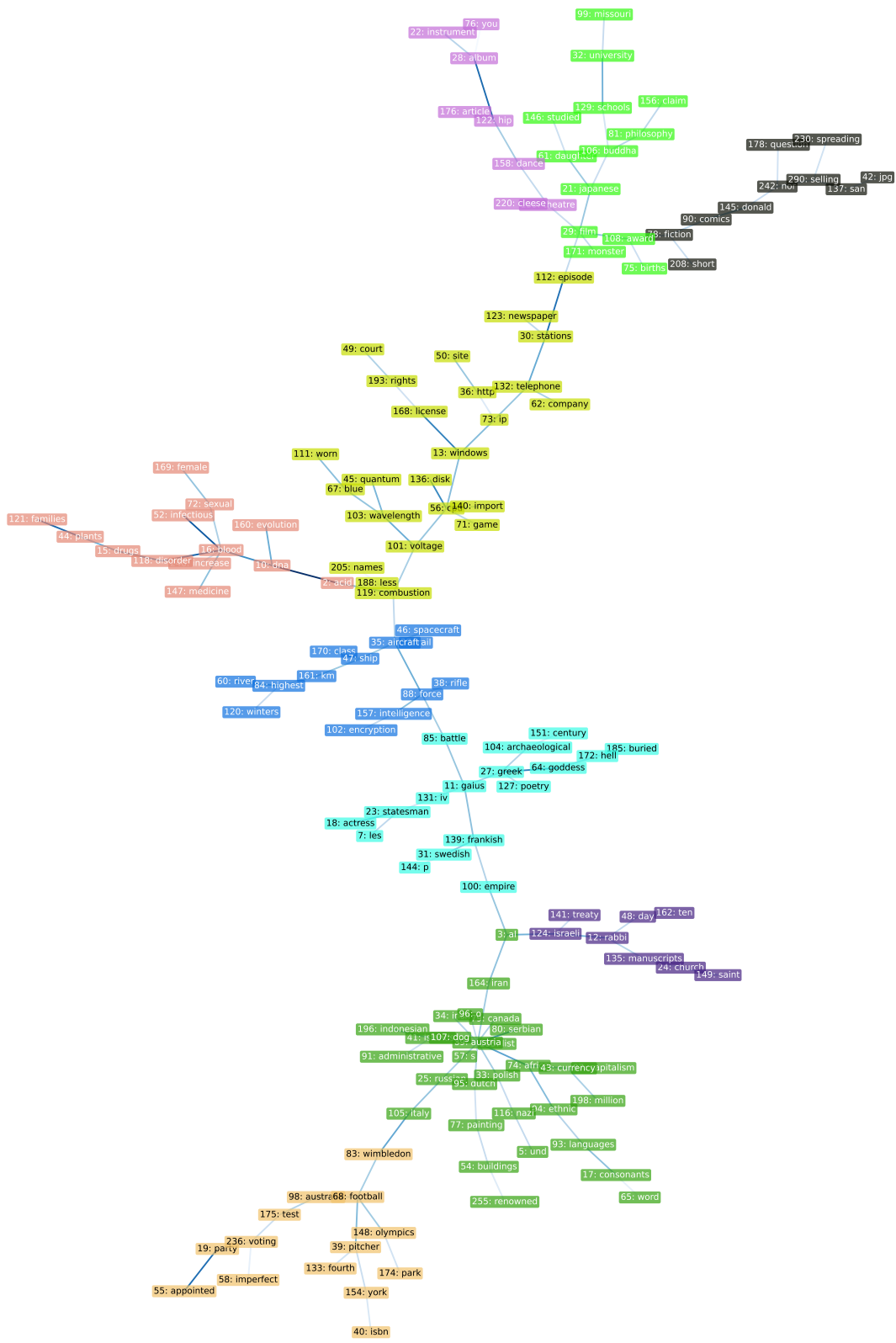


Figure 12: Visualization of the entire MST T_{150} defined in Sec. 5. Each color of the nodes represents one of the ten clusters obtained by Spectral Clustering.

$E(S_{63}^2, S_{210}^2) = 2.964$ Axis 63 Axis 210	$E(S_{10}^2, S_{125}^2) = 2.431$ Axis 10 Axis 125	$E(S_{14}^2, S_{113}^2) = 2.380$ Axis 14 Axis 113	$E(S_{63}^2, S_{184}^2) = 2.330$ Axis 63 Axis 184
organization unesco international itu organizations interpel interpel observer	acid morphisms hydrogen homomorphism acids hydrogen oh wavelengths	dna algae rna bacteria mrna fungi mitochondria	imperfect accusative perfect nouns future genitive present noun
$E(S_{2}^2, S_{10}^2) = 2.323$ Axis 2 Axis 10	$E(S_{22}^2, S_{59}^2) = 2.247$ Axis 22 Axis 59	$E(S_{26}^2, S_{134}^2) = 2.233$ Axis 26 Axis 134	$E(S_{14}^2, S_{114}^2) = 2.228$ Axis 14 Axis 114
acid dna hydrogen proteins acids rna oh mrna	instrument concerto instruments fugue bass sonata guitars bwv	cars prix ford grand car schumacher chassis race	topological morphisms isomorphic homomorphism hydrogen hydrogen topology wavelengths
$E(S_{10}^2, S_{114}^2) = 2.150$ Axis 10 Axis 114	$E(S_{16}^2, S_{118}^2) = 2.124$ Axis 16 Axis 118	$E(S_{1}^2, S_{121}^2) = 2.107$ Axis 1 Axis 121	$E(S_{28}^2, S_{122}^2) = 2.086$ Axis 28 Axis 122
dna morphisms proteins homomorphism rna hydrogen mrna wavelengths	blood disorder organs mental hydrogen disorders kidney symptoms	genus families species family extinct older birds household	plants families plant family flowers older flowering household
$E(S_{30}^2, S_{112}^2) = 2.060$ Axis 30 Axis 112	$E(S_{6}^2, S_{96}^2) = 2.032$ Axis 6 Axis 96	$E(S_{21}^2, S_{110}^2) = 2.028$ Axis 21 Axis 110	$E(S_{13}^2, S_{168}^2) = 1.991$ Axis 13 Axis 168
stations episode fm aired radio show broadcast tv	el o spanish portuguese nacional paulo jos rio	japanese martial japan judo tokyo aikido emperor karate	greek goddess greece gods athens deity athenian deities
$E(S_{12}^2, S_{66}^2) = 1.975$ Axis 12 Axis 66	$E(S_{4}^2, S_{106}^2) = 1.974$ Axis 4 Axis 106	$E(S_{56}^2, S_{136}^2) = 1.967$ Axis 56 Axis 136	$E(S_{17}^2, S_{114}^2) = 1.966$ Axis 17 Axis 114
rabbi judah talmud israelites rabbin yahveh torah elisha	india buddha indian buddhism nehru mahayana hindu buddhist	cpu disk microprocessor floppy processor disks cpus drives	consonants morphisms vowels homomorphism vowel hydrogen consonant wavelengths
$E(S_{0}^2, S_{82}^2) = 1.927$ Axis 0 Axis 82	$E(S_{53}^2, S_{150}^2) = 1.915$ Axis 53 Axis 150	$E(S_{80}^2, S_{89}^2) = 1.909$ Axis 80 Axis 89	$E(S_{39}^2, S_{51}^2) = 1.885$ Axis 39 Axis 51
dishes beer sauce beers fried ale dish brewing	element nuclear metals bomb elements bombs uranium fission	serbian austria serbia belgium serbia luxembourg croatia germany	pitcher coach sox quarterback baseman defensive pitchers bengals
$E(S_{53}^2, S_{86}^2) = 1.872$ Axis 53 Axis 86	$E(S_{39}^2, S_{128}^2) = 1.871$ Axis 39 Axis 128	$E(S_{6}^2, S_{173}^2) = 1.869$ Axis 6 Axis 173	$E(S_{56}^2, S_{126}^2) = 1.861$ Axis 56 Axis 126
element rocks metals volcanic elements granite uranium geologic	pitcher ball sox scrimmage baseball goal pitchers foul	el basque spanish china nacional aragon jos eta	cpu pointer microprocessor return processor string cpus pointers
$E(S_{74}^2, S_{89}^2) = 1.854$ Axis 74 Axis 89	$E(S_{15}^2, S_{16}^2) = 1.834$ Axis 15 Axis 16	$E(S_{83}^2, S_{105}^2) = 1.832$ Axis 83 Axis 105	$E(S_{17}^2, S_{233}^2) = 1.828$ Axis 17 Axis 233
africa austria african belgium africans luxembourg namibia germany	drugs blood drug organs heroin liver lsd kidney	wimbledon italy open norway finalist netherlands quarter germany	consonants hong vowels kong vowel guidance consonant mine
$E(S_{30}^2, S_{132}^2) = 1.820$ Axis 30 Axis 132	$E(S_{10}^2, S_{160}^2) = 1.811$ Axis 10 Axis 160	$E(S_{86}^2, S_{195}^2) = 1.809$ Axis 86 Axis 195	$E(S_{101}^2, S_{103}^2) = 1.800$ Axis 101 Axis 103
stations telephone fm phone radio mobile broadcast cellular	dna evolution proteins evolutionary ma darwin mrna selection	rocks cretaceous volcanic geologic granite epoch geologic extinction	voltage wavelength electrical light circuits wavelengths current laser
$E(S_{107}^2, S_{138}^2) = 1.793$ Axis 107 Axis 138	$E(S_{15}^2, S_{44}^2) = 1.793$ Axis 15 Axis 44	$E(S_{32}^2, S_{129}^2) = 1.793$ Axis 32 Axis 129	$E(S_{3}^2, S_{124}^2) = 1.786$ Axis 3 Axis 124
dog horse hound horses dogs riding breed breed	drugs plants drug plant heroin flowers lsd flowering	university schools college school technology secondary institute education	stars spacecraft constellation nasa star astronauts constellations astronaut
$E(S_{14}^2, S_{113}^2) = 2.380$ Axis 14 Axis 113	$E(S_{63}^2, S_{184}^2) = 2.330$ Axis 63 Axis 184	$E(S_{2}^2, S_{10}^2) = 2.323$ Axis 2 Axis 10	$E(S_{14}^2, S_{114}^2) = 2.228$ Axis 14 Axis 114
topological frac isomorphic cos banach equation topology euler	organization g international e organizations icao interpel fao	acid element hydrogen metals acids elements oh uranium	blood infectious organs infection liver disease kidney infections
$E(S_{10}^2, S_{114}^2) = 2.150$ Axis 10 Axis 114	$E(S_{16}^2, S_{118}^2) = 2.124$ Axis 16 Axis 118	$E(S_{1}^2, S_{121}^2) = 2.107$ Axis 1 Axis 121	$E(S_{28}^2, S_{122}^2) = 2.086$ Axis 28 Axis 122
dna morphisms proteins homomorphism rna hydrogen mrna wavelengths	blood disorder organs mental hydrogen disorders kidney symptoms	genus families species family extinct older birds household	album hip albums hop band dj songs rap
$E(S_{30}^2, S_{112}^2) = 2.060$ Axis 30 Axis 112	$E(S_{6}^2, S_{96}^2) = 2.032$ Axis 6 Axis 96	$E(S_{21}^2, S_{110}^2) = 2.028$ Axis 21 Axis 110	$E(S_{13}^2, S_{168}^2) = 1.991$ Axis 13 Axis 168
stations episode fm aired radio show broadcast tv	el o spanish portuguese nacional paulo jos rio	japanese martial japan judo tokyo aikido emperor karate	greek goddess greece gods athens deity athenian deities
$E(S_{12}^2, S_{66}^2) = 1.975$ Axis 12 Axis 66	$E(S_{4}^2, S_{106}^2) = 1.974$ Axis 4 Axis 106	$E(S_{56}^2, S_{136}^2) = 1.967$ Axis 56 Axis 136	$E(S_{17}^2, S_{114}^2) = 1.966$ Axis 17 Axis 114
rabbi judah talmud israelites rabbin yahveh torah elisha	india buddha indian buddhism nehru mahayana hindu buddhist	cpu disk microprocessor floppy processor disks cpus drives	consonants morphisms vowels homomorphism vowel hydrogen consonant wavelengths
$E(S_{0}^2, S_{82}^2) = 1.927$ Axis 0 Axis 82	$E(S_{53}^2, S_{150}^2) = 1.915$ Axis 53 Axis 150	$E(S_{80}^2, S_{89}^2) = 1.909$ Axis 80 Axis 89	$E(S_{39}^2, S_{51}^2) = 1.885$ Axis 39 Axis 51
dishes beer sauce beers fried ale dish brewing	element nuclear metals bomb elements bombs uranium fission	serbian austria serbia belgium serbia luxembourg croatia germany	pitcher coach sox quarterback baseman defensive pitchers bengals
$E(S_{53}^2, S_{86}^2) = 1.872$ Axis 53 Axis 86	$E(S_{39}^2, S_{128}^2) = 1.871$ Axis 39 Axis 128	$E(S_{6}^2, S_{173}^2) = 1.869$ Axis 6 Axis 173	$E(S_{56}^2, S_{126}^2) = 1.861$ Axis 56 Axis 126
element rocks metals volcanic elements granite uranium geologic	pitcher ball sox scrimmage baseball goal pitchers foul	el basque spanish china nacional aragon jos eta	cpu pointer microprocessor return processor string cpus pointers
$E(S_{74}^2, S_{89}^2) = 1.854$ Axis 74 Axis 89	$E(S_{15}^2, S_{16}^2) = 1.834$ Axis 15 Axis 16	$E(S_{83}^2, S_{105}^2) = 1.832$ Axis 83 Axis 105	$E(S_{17}^2, S_{233}^2) = 1.828$ Axis 17 Axis 233
africa austria african belgium africans luxembourg namibia germany	drugs blood drug organs heroin liver lsd kidney	wimbledon italy open norway finalist netherlands quarter germany	consonants hong vowels kong vowel guidance consonant mine
$E(S_{30}^2, S_{132}^2) = 1.820$ Axis 30 Axis 132	$E(S_{10}^2, S_{160}^2) = 1.811$ Axis 10 Axis 160	$E(S_{86}^2, S_{195}^2) = 1.809$ Axis 86 Axis 195	$E(S_{101}^2, S_{103}^2) = 1.800$ Axis 101 Axis 103
stations telephone fm phone radio mobile broadcast cellular	dna evolution proteins evolutionary ma darwin mrna selection	rocks cretaceous volcanic geologic granite epoch geologic extinction	voltage wavelength electrical light circuits wavelengths current laser
$E(S_{107}^2, S_{138}^2) = 1.793$ Axis 107 Axis 138	$E(S_{15}^2, S_{44}^2) = 1.793$ Axis 15 Axis 44	$E(S_{32}^2, S_{129}^2) = 1.793$ Axis 32 Axis 129	$E(S_{3}^2, S_{124}^2) = 1.786$ Axis 3 Axis 124
dog horse hound horses dogs riding breed breed	drugs plants drug plant heroin flowers lsd flowering	university schools college school technology secondary institute education	stars spacecraft constellation nasa star astronauts constellations astronaut

Table 7: Complementary experimental results to Table 1. The top 60 pairs with the highest $E(S_i^2, S_j^2)$ values are presented. For each component, the top 4 words with the largest component values are listed.

$E(S_{10}^2 S_{10}^2) = 2.323$		$E(S_{19}^2 S_{19}^2) = 1.755$		$E(S_{30}^2 S_{30}^2) = 1.820$		$E(S_{73}^2 S_{73}^2) = 1.693$		$E(S_{62}^2 S_{62}^2) = 1.632$		$E(S_{56}^2 S_{56}^2) = 1.967$	
Axis 2	Axis 10	Axis 2	Axis 119	Axis 132	Axis 30	Axis 132	Axis 73	Axis 132	Axis 62	Axis 136	Axis 56
acid	dna	acid	combustion	telephone	stations	telephone	ip	telephone	company	disk	cpu
hydrogen	proteins	hydrogen	diesel	phone	fm	phone	tcp	phone	corporation	floppy	microprocessor
acids	rna	acids	turbine	mobile	radio	mobile	protocols	mobile	corporation	disks	processor
oh	mna	oh	engine	cellular	broadcast	cellular	protocol	cellular	shareholders	drives	cpus
w_k	$S_{k,2}^2 S_{k,10}^2$	w_k	$S_{k,2}^2 S_{k,119}^2$	w_k	$S_{k,132}^2 S_{k,30}^2$	w_k	$S_{k,132}^2 S_{k,73}^2$	w_k	$S_{k,132}^2 S_{k,62}^2$	w_k	$S_{k,136}^2 S_{k,56}^2$
ribose	3755.7	pyrolysis	2794.4	digitalized	4726.8	multipoint	2062.7	esat	3145.5	sata	3427.5
deoxyribose	2963.9	syngas	2056.9	arabsat	4657.2	pstn	1996.9	telecoms	2547.9	udma	2519.7
phosphodiester	2850.2	gasification	1783.5	radiotelephone	4453.9	wimax	1873.8	nynex	2155.9	backplanes	2008.9
biosynthesis	2510.1	butane	1761.2	landlines	3522.1	xdsl	1491.2	gnc	1810.0	nextgen	1947.7
methyltransferase	2482.9	dehydrogenation	1623.0	intersputnik	3053.5	svcs	1361.2	hätel	1657.3	megabytes	1890.1
pyrimidine	2399.6	tert	1230.2	telex	2722.4	isdn	1235.8	openreach	1529.2	eisa	1859.5
$E(S_{16}^2 S_{16}^2) = 1.947$		$E(S_{160}^2 S_{160}^2) = 1.811$		$E(S_{56}^2 S_{56}^2) = 1.615$		$E(S_{56}^2 S_{56}^2) = 1.732$		$E(S_{168}^2 S_{168}^2) = 1.991$		$E(S_{73}^2 S_{73}^2) = 1.740$	
Axis 10	Axis 16	Axis 10	Axis 160	Axis 140	Axis 56	Axis 13	Axis 56	Axis 13	Axis 168	Axis 13	Axis 73
dna	blood	dna	evolution	import	cpu	windows	cpu	windows	license	windows	ip
proteins	organs	proteins	evolutionary	duplicate	microprocessor	os	microprocessor	os	copyleft	os	tcp
rna	liver	rna	darwin	info	processor	unix	processor	unix	gpl	unix	protocols
mna	kidney	mna	selection	no	cpus	linux	cpus	linux	licenses	linux	protocol
w_k	$S_{k,10}^2 S_{k,16}^2$	w_k	$S_{k,10}^2 S_{k,160}^2$	w_k	$S_{k,140}^2 S_{k,56}^2$	w_k	$S_{k,13}^2 S_{k,56}^2$	w_k	$S_{k,13}^2 S_{k,168}^2$	w_k	$S_{k,13}^2 S_{k,73}^2$
adenylate	2079.8	utr	2381.5	superpipelined	5652.9	xcode	2609.2	qpl	5678.2	netware	1799.2
effectors	1842.5	reticulum	1942.0	strongarm	3220.2	powerpc	2046.7	lgpl	4519.9	netbios	1543.2
antisense	1639.9	genomic	1668.6	speccrate	2470.5	itanium	1500.1	trolltech	3588.4	imap	1414.0
cyclase	1638.9	homozygous	1599.1	specbaseate	1524.5	glibc	1355.2	gpl	1432.6	glut	1239.0
myosin	1201.8	cleaved	1181.0	insubstantial	1387.8	irix	1177.1	gnu	2826.1	wfww	1179.9
axons	1144.2	tubulin	1152.4	eisa	1027.8	efi	1161.1	bsd	2822.7	dhcpv	1115.5
$E(S_{118}^2 S_{118}^2) = 1.959$		$E(S_{44}^2 S_{44}^2) = 1.793$		$E(S_{248}^2 S_{248}^2) = 1.499$		$E(S_{147}^2 S_{147}^2) = 1.717$		$E(S_{72}^2 S_{72}^2) = 1.628$		$E(S_{52}^2 S_{52}^2) = 2.158$	
Axis 15	Axis 118	Axis 15	Axis 44	Axis 16	Axis 248	Axis 16	Axis 147	Axis 16	Axis 72	Axis 16	Axis 52
drugs	disorder	drugs	plants	blood	increase	blood	medicine	blood	sexual	blood	infectious
drug	mental	drug	plant	organs	increased	organs	medical	organs	sex	organs	infection
heroin	disorders	heroin	flowers	liver	increasing	liver	doctors	liver	homosexual	liver	disease
lsd	symptoms	lsd	flowering	kidney	increases	kidney	care	kidney	heterosexual	kidney	infections
w_k	$S_{k,15}^2 S_{k,118}^2$	w_k	$S_{k,15}^2 S_{k,44}^2$	w_k	$S_{k,16}^2 S_{k,248}^2$	w_k	$S_{k,16}^2 S_{k,147}^2$	w_k	$S_{k,16}^2 S_{k,72}^2$	w_k	$S_{k,16}^2 S_{k,52}^2$
adhd	3505.8	peyote	3197.5	esophagus	2274.6	aortic	1726.9	erectile	2001.5	abscess	1932.6
anticonvulsants	3047.9	purpura	2926.6	lobes	1462.4	brainstem	1537.1	dildo	1788.8	multifocal	1440.2
sertraline	2374.6	meo	2878.6	cava	1360.8	endoscopy	1533.7	clitoral	1481.5	hemorrhagic	1239.3
lorazepam	1604.8	delirians	2397.0	ligamentum	1024.8	laparoscopic	1509.4	deferens	1432.6	esophagitis	1187.4
anticonvulsant	1487.1	diplopterys	2395.1	transversal	1011.2	angioplasty	1447.4	rectal	1352.0	efferent	1160.5
somnolence	1426.1	cabrerana	2237.7	vena	1005.6	cardiology	1433.3	urogenital	1344.7	mitral	1143.5
$E(S_{118}^2 S_{118}^2) = 2.124$		$E(S_{112}^2 S_{112}^2) = 2.060$		$E(S_{123}^2 S_{123}^2) = 1.570$		$E(S_{50}^2 S_{50}^2) = 1.688$		$E(S_{73}^2 S_{73}^2) = 1.419$		$E(S_{193}^2 S_{193}^2) = 1.495$	
Axis 16	Axis 118	Axis 30	Axis 112	Axis 30	Axis 123	Axis 36	Axis 50	Axis 36	Axis 73	Axis 168	Axis 193
blood	disorder	stations	episode	stations	newspaper	http	site	http	http	license	rights
organs	mental	fm	aired	fm	daily	www	website	www	tcp	copyleft	legislation
liver	disorders	radio	show	radio	weekly	htm	forum	htm	protocols	gpl	act
kidney	symptoms	broadcast	tv	broadcast	newspapers	html	photos	html	protocol	licenses	laws
w_k	$S_{k,16}^2 S_{k,118}^2$	w_k	$S_{k,30}^2 S_{k,112}^2$	w_k	$S_{k,30}^2 S_{k,123}^2$	w_k	$S_{k,36}^2 S_{k,50}^2$	w_k	$S_{k,36}^2 S_{k,73}^2$	w_k	$S_{k,168}^2 S_{k,193}^2$
atrophy	2110.2	rebroadcast	1729.4	canwest	1941.7	shtml	1537.9	mtu	1425.4	copyleft	1648.0
hemiparesis	1877.5	fsn	1635.4	ctv	1343.4	geocities	1230.3	stateful	1352.4	magnatune	1131.9
axonal	1465.9	etv	1600.9	wqxr	1276.0	jeancocteau	871.2	proxying	1324.2	rightsholder	839.7
dysfunction	1380.2	upn	1534.6	superstation	1144.2	lfc	758.0	mpls	1264.5	redistribute	809.7
neuropathy	1300.1	wxyz	1441.3	wanbao	1116.1	uchicago	644.7	vpns	798.6	copyrights	676.5
myopathy	1288.3	whdh	1392.0	aor	998.0	archivo	593.3	kleinrock	796.1	circumvention	653.3
$E(S_{221}^2 S_{221}^2) = 1.701$		$E(S_{121}^2 S_{121}^2) = 2.096$		$E(S_{103}^2 S_{103}^2) = 1.765$		$E(S_{193}^2 S_{193}^2) = 1.616$		$E(S_{101}^2 S_{101}^2) = 1.693$			
Axis 169	Axis 72	Axis 44	Axis 121	Axis 45	Axis 103	Axis 49	Axis 193	Axis 56	Axis 101		
female	sexual	plants	families	quantum	wavelength	court	rights	cpu	voltage		
male	sex	plant	family	particles	light	judge	legislation	microprocessor	electrical		
age	homosexual	flowers	older	particle	wavelengths	courts	act	processor	circuits		
infant	heterosexual	flowering	household	physics	laser	trial	laws	cpus	current		
w_k	$S_{k,169}^2 S_{k,72}^2$	w_k	$S_{k,44}^2 S_{k,121}^2$	w_k	$S_{k,45}^2 S_{k,103}^2$	w_k	$S_{k,49}^2 S_{k,193}^2$	w_k	$S_{k,56}^2 S_{k,101}^2$		
male	1240.5	rosid	4158.0	mesons	3078.7	habeas	954.7	lsi	2589.8		
vulval	1191.4	caryophyllales	4064.1	gluons	2079.4	declaratory	823.5	microelectronic	2081.5		
faggot	981.2	dicotyledons	3652.5	photon	1648.3	conservatorship	783.1	sram	1901.2		
spermatozoon	961.5	betulaceae	3637.6	photons	1567.6	waives	753.2	mosfet	1757.0		
frot	940.6	cronquist	3636.1	synchrotron	1435.1	laches	734.4	voltages	1582.9		
tribadism	843.5	poaceae	3295.0	isospin	1414.1	talionis	721.3	microcontrollers	1554.5		

Table 9: Complementary experimental results to Table 3. For all component pairs (S_i, S_j) in the second subtree of the MST in Fig. 5, the top 6 words and their corresponding $S_{i,i}^2 S_{j,j}^2$ values that contribute the most to the $E(S_i^2 S_j^2)$ value are presented.